Inclusion of Ash and SO_2 emissions from volcanic eruptions in WRF-Chem: Development and some applications

M. Stuefer[1], S. R. Freitas[2], G. Grell[3], P. Webley[1], S. Peckham[3], S. A. McKeen[3], and S. D. Egan[1]

1) Geophysical Institute, University of Alaska Fairbanks, 903 Koyukuk Drive, Fairbanks, AK 99775 USA.
[2] Center for Weather Prediction and Climate Studies - CPTEC/INPE, Cachoeira Paulista, São Paulo, Brazil, 12630-000
[3] National Oceanic and Atmospheric Administration Earth Systems Research Laboratory, 325 Broadway, Boulder, CO 80305-3337

Corresponding author
Martin Stuefer
Geophysical Institute,
University of Alaska Fairbanks, 903 Koyukuk Drive,
Fairbanks, Alaska 99775-7320
email: stuefer@gi.alaska.edu
Phone: +1 907 474 6477
Fax: +1 907 474 7290

Abstract

We describe a new functionality within the Weather Research and Forecasting model with coupled Chemistry (WRF-Chem) that allows simulating emission, transport, dispersion, transformation and sedimentation of pollutants released during volcanic activities. Emissions from both an explosive eruption case and relatively calm degassing situation are considered using the most recent volcanic emission databases. A preprocessor tool provides emission fields and additional information needed to establish the initial three-dimensional cloud umbrella/vertical distribution within the transport model grid, as well as the timing and duration of an eruption. From this source condition, the transport, dispersion and sedimentation of the ash-cloud can be realistically simulated by WRF-Chem using its own dynamics, physical parameterization as well as data assimilation. Examples of model validation include a comparison of tephra fall deposits from the 1989 eruption of Mount Redoubt (Alaska), and the dispersion of ash from the 2010 Eyjafjallajökull eruption in Iceland. Both model applications show good coincidence between WRF-Chem and observations.

Keywords: WRF-Chem, Volcano, Ash Clouds, Extreme Aerosol, Volcanic SO_2

1. Introduction

Past and recent volcanic eruptions, such as Eyjafjallajökull (Gudmundsson et al., 2010) and Puyehue Cordon-Caulle (BGVM, 2011), with huge impacts on the environment (soil, water), air quality and air traffic have been increasing the need of accurate real time forecasts of ash movement and sedimentation and others hazardous products. Currently, most existing volcanic ash transport and dispersion (VATD) models involve a de-coupled or 'offline' treatment of the physics and chemistry characterizing atmospheric-dispersion of volcanic emissions, and numerical weather prediction. See WMO (2010) for a report on the various available VATD models. However, interactions between the erupting plume and surrounding meteorological conditions could significantly affect the settling of volcanic ash/aerosol particles. As a consequence, inaccurate handling of atmospheric processes and a loss of important feedback processes between atmosphere and pollutants might result. Grell and Baklanov (2011) emphasize the differences between offline and online approaches for both air quality and numerical weather prediction. In general operational prediction centers use de-coupled offline models due to the low computational cost. However, with the fast increase in computing power, integrated modeling systems become more and more popular. Online models account for inclusion of two-way interactions of physical and chemical atmospheric processes. The weather is the main factor for air quality, and on the other hand, chemical species may influence weather due to radiative effects or changes in cloud microphysics. These effects are most pronounced for high aerosol concentrations during the extreme events of volcanic eruptions or large wildfire emissions into the atmosphere. Grell et al (2011) demonstrated that aerosol feedback processes calculated within the online modeling approach induced considerable improved meteorological fields during the extreme 2004-wildfire season in Alaska. During such intense aerosol events it is easy to show that online models represent the atmosphere more realistically. Errors in air quality prediction introduced by the offline approach can be quite

substantial especially as the model resolution is increased (Grell and Baklanov 2011). The online approach using models such as the Weather Research and Forecasting (WRF) with Chemistry (WRF-Chem, Grell et al. 2005) accounts for a numerical consistent air quality forecast; no interpolation in time or space is required. In this paper, we describe how volcanic emissions may be included in WRF-Chem and apply the model using emissions from volcanic eruptions. We use WRF-Chem for studies of past volcanic eruptions to better understand volcanic emissions and their transport within the atmosphere. The modeled feedback between volcanic emissions is suitable for climate impact studies and for detailed studies of the dispersion and the weather following an eruption event. In the following, we describe the implementation of generalized volcanic source parameters within WRF-Chem indicating an opportunity to use the modeling system for near-real time eruptions at times during an event when the user might know a location and maybe the height of a volcanic plume, but otherwise there is little information available about the characteristics of a certain eruption. WRF-Chem is based on the WRF model (Skamarock et al. 2005). The architecture of WRF supports both research and operational weather forecasting applications. WRF includes various options for dynamic cores and physical parameterizations (Skamarock et al. 2005) so that it can be used to simulate atmospheric processes over a wide range of spatial and temporal scales. WRF-Chem simulates trace gases and particulates interactively with the meteorological fields using several treatments for photochemistry and aerosols developed by the user community. The work described in this paper is based on WRF version 3.3.1 and 3.4 (WRFV3.4), released in April of 2012. A brief description is given at the beginning of section 3.

Section 2 of this paper describes the source parameters that we use to determine volcanic emissions, as well as sulfur dioxide (SO_2) from volcanic degassing processes. In Section 3, we explain the implementation into WRF-Chem. Section 4

demonstrates two applications. Section 5 discusses some of the software issues. Our conclusions are discussed in section 6.

2. Volcanic emissions

Volcanic ash, SO_2 and other trace gases, are perturbing atmospheric composition and chemistry. Volcanic ash is typically composed of fine-grained rock, mineral fragments, and glass shards generated during eruptions. With any VATD model and especially WRF-Chem, initial source information on the volcanic emissions is critical for the model's ability to forecast the ash cloud movement and provide warnings on actual ashfall concentrations (Webley and Mastin, 2009). A volcanic plume model generates the source data for WRF-Chem. The necessary parameters are the scale of the eruption including the erupted mass, the initial altitudes of the ash particles and SO_2, an eruption rate, and a grain size spectrum of the ash particles. Mastin et al. (2009) have developed 'Eruption Source Parameters (ESP)' for the world's volcanoes. Each of the world's volcanoes has a 'typical' eruption assigned to them. Mastin et al. (2009) provide details on each source parameter for each ESP type, which include plume altitude, mass of the eruption cloud and particle size distributions. WRF-Chem uses the ESP type data as volcanic emission information for the model forecasting. The modeled volcanic ash is subdivided into 10 different bins representing the size spectrum of the particles typically ranging from a few micrometers up to one or two millimeters. We have developed a volcanic emissions preprocessor for initializing the ash fields within the model based on a look-up table containing the ESP data. The programming code of the Coupled Aerosol-Tracer Transport model, which has been developed for the Brazilian version of the Regional Atmospheric Modeling System (Freitas et al., 2009), has been used as a template and adapted to suit WRF-Chem. In the following subsection we describe how ash and SO_2 emissions from volcanic activities are formulated for use in the WRF-Chem model.

2.1. The emissions preprocessor

To determine eruption source parameters during volcanic eruption events, we use an emission-preprocessing tool (Freitas et al., 2011) following the database developed by Mastin et al. (2009). This database provides a set of parameters to model volcanic ash cloud transport and dispersion during eruptions. There is information on 1535 volcanoes around the world comprising location (latitude, longitude and height) as well as the corresponding historical parameters of plume height, mass eruption rate, volume rate, duration of eruption and the mass fraction of erupted debris finer than about 63 μm (see Table 1). Note that all parameters from this default database may be overwritten by the user once more accurate information is available. The emissions preprocessing tool provides the location of the volcano in the nearest model grid box and the emission parameters (i.e. mass eruption rate, plume height and time duration), if no other observations are given. This information is used within WRF-Chem to determine the vertical distribution of the erupted mass. Large volcanic plumes are typically 'umbrella' shaped (Sparks, 1997), i.e. their vertical distribution is shaped as detailed in Fig. 1. We use this observation - which may be modified by users - and assume that 75% of the erupted mass is detrained in the umbrella cloud and 25% beneath, with a linear distribution from the umbrella to the vent. The base of the umbrella cloud is roughly located at 73% of the plume height. Figure 1 shows an example of the vertical profile of the ash-cloud mass distribution associated with an eruption with 12 km height above the vent, while the cloud base is located around 9 km height above it. Note the umbrella cloud detrainment layer is represented as a parabolic mass distribution with 75% of the erupted mass. Twenty-five percent of the erupted mass is linearly detrained from the umbrella base to the vent height. Note that this method does not account for the detailed dynamics of the erupted plume above the volcano vent; we further do not include any data on the

thermodynamics of the eruption itself. Phenomena such as pyrocumuli are not resolved within the model. Data on atmospheric heat release during an eruption, or detailed plume dynamics are very sparse. The total erupted mass is calculated using the corresponding erupted volume (Table 1) times the ash mass density, which is defined as 2,600 kg m^{-3}. Then the total ash mass is distributed between 10 bins of aerosol particles with diameter size range starting from 2 mm down to less than 3.9 μm, using the corresponding percentage of mass derived from analysis of historic eruptions. Table 2 gives the selected particle size bins, which have been associated with the WRF-Chem variable names vash_1 to vash_10, and the corresponding mass fraction percentage for each volcano ESP type. Scollo et al. (2007), Rose et al. (2007), Durant and Rose (2009), Bonadonna and Houghton (2005), Durant et al. (2009), and Bonadonna et al. (2002) used analysis of ash samples mostly from the example eruptions listed in Table 1 to derive the mass fraction percentage shown in Table 2. For each bin, the aerodynamic radius, needed by the settling velocity calculation, is defined as half of the arithmetic mean between the limits of the diameters of each bin size. The time interval during which the ash mass is released in the domain of the model simulation is given by the default 'duration' parameter as specified in Table 1. If observed data of injection height *h* and eruption length *d* are available, they may be used instead. The 1535 volcanoes with referenced source parameters as specified in Table 1, for which WRF-Chem is able to simulate the associated ash-cloud movement in an event of eruption, are shown in Figure 2. This figure shows the geographical location in the world and also depicts the prescribed plume height above the vent.

2.2 Volcanic SO_2 degassing emissions

The data provided by the AEROCOM program (http://www-lscedods.cea.fr/aerocom/AEROCOM_HC/volc/, Diehl, 2009, Diehl et al., 2012) contains volcanic SO_2 emissions and other variables for all days from 1 January 1979 to 31 December 2009 for all volcanoes with historic eruptions listed in the

Global Volcanism Program database provided by the Smithsonian Institution. There is one file for each year that contains the number of events for each day of that year over the entire world. For each event the volcano name, date, height above the mean sea level, cloud column height, longitude, latitude and daily emission rate of SO_2 are provided. There is also a separation between eruptive and non-eruptive volcanic emissions.

In similar fashion to the volcanic ash, the emissions processing tool places the SO_2 emissions from each volcano in the grid box, which surrounds its geographical location. The total emission is calculated by summing the emissions of all volcanoes within the grid cell. Next, the total emission and the minimum and maximum column heights of the set of volcanoes within the grid cell are provided. The units are kg [SO_2] m^{-2} dy^{-1}. If other observed volcanic SO_2 emission data are available (i.e. from satellite retrievals using the Ozone Monitoring Instrument), or SO_2 emissions are modeled for volcanic eruptions outside the date range covered by the AEROCOM data, SO_2 mass emission rates can be entered in the WRF-Chem emissions driver. In this case the SO_2 plume resembles the umbrella shaped plume of the emitted ash as described above.

In general, once airborne, SO_2 oxidizes to sulfuric acid (H_2SO_4) that condenses into sulfate aerosol, and the atmospheric loading and residence time of the sulfate aerosol is proportional to the sulfur-containing gases in the volcanic plume. As for the ash emissions, -to evaluate the impacts of volcanic emissions, it is important to use accurate assumptions not only of SO_2 emission rates, but also of injection heights. It is important to note that SO_2 may show different plume characteristics than volcanic ash; also the residence time of sulfate aerosol may differ significantly from the residence time of ash. An example was the June 1991 eruption of Pinatubo (Philippines), which injected large amounts of SO_2 and ash up to 35 km (ASL) into

the stratosphere. The sulfate aerosol was detected for many months after the eruption, while the ash settled within several days (McCormick et al., 1995).

3. Inclusion of volcanic emissions in WRF-Chem

In this section we describe how ash and SO_2 emissions from volcanic activities are used in the WRF-Chem model. WRF/Chem v3.4 contains two hard coded gas-phase chemical mechanisms: the second generation Regional Acid Deposition Model Mechanism (RADM2) (Stockwell et al., 1990), and the Carbon-Bond Mechanism version Z (CBM-Z) (Zaveri and Peters, 1999). The Kinetic PreProcessor (KPP, Salzmann, 2008, Grell et al., 2011) is also used in WRF-Chem, which allows many additional gas-phase chemical mechanisms. The three aerosol modules available in WRFV3.4 are the Modal Aerosol Dynamics Model for Europe (MADE) (Ackermann et al., 1998) with the secondary organic aerosol (SOA) model (SORGAM) of Schell et al. (2001) (referred to as MADE/SORGAM), and the Model for Simulating Aerosol Interactions and Chemistry (MOSAIC) (Zaveri et al., 2008). The Volatility Basis Set (VBS) approach has been coupled to both, MOSAIC (Shrivastava et al., 2011) and MADE (Ahmadov et al., 2012). The numerically very simple and computationally inexpensive bulk approach from the Goddard Chemistry Aerosol Radiation and Transport (GOCART, Chin et al., 2002) model is also available in WRF-Chem V3.4. An aerosol optical property module (Fast et al., 2006, Barnard et al., 2010) was added to WRF-Chem that treats bulk, modal, and sectional aerosol size distribution using a similar methodology for refractive indices and multiple mixing rules. The WRF-Chem aerosol modules allow for quantification of the interaction between aerosol and precipitation, such as the first aerosol indirect effect (Twomey, 1977) referring to the modification of the cloud droplet number concentration by aerosols, or the second indirect effect, which was first proposed by Albrecht (1989), who showed that the suppression of precipitation by aerosols could increase cloud water content (or cloud liquid water

path, LWP) and fractional cloud cover. The interactions between aerosols and clouds, such as the first and second indirect effects, activation/resuspension, wet scavenging, and aqueous chemistry are described in more detail by Gustafson et al. (2007) and Chapman et al. (2009).

For the initial release in the modeling system, the user may use volcanic emissions with several chemistry options. Three main options to characterize volcanic ash are available. The simplest and computationally least expensive approach is to use (1) the four finest ash species as invariant tracers that are being transported, deposited and settled only. A further option allows (2) selecting a number of 10 ash variables, which also includes coarse ash species for estimates of ash fall. The third option (3) distinguishes only 2 different ash species by including the ash within the WRF-Chem particulate variables; this option enables the user to take advantage of all aerosol feedback processes implemented within WRF-Chem.

(1) When simulating ash as an invariant tracer using 4 ash variables and no chemistry modules, only settling is applied and dry deposition is neglected, since the settling effect is much stronger for these fairly heavy particles. Wet deposition uses a simple scavenging rate of 0.5, applied both for parameterized and large-scale precipitation. The algorithm to calculate the settling velocity was originally developed for the GOCART model (Chin et al., 2002), but modified here for aerodynamic radius and ash mass density. The calculation is based on the Stokes law corrected by the Cunningham slip factor (Pruppacher and Klett, 1997). This option may be useful for quick emergency simulations for aviation purposes. An example would be the Eyjafjallajökull eruption as described below. Computational cost is minimal, since no chemistry is involved and additional computations are derived mostly from advective transport of the 4 additional variables.

(2) The next step up is to use the full 10 particle size bins. This option is useful if ash-fall is important to predict with reasonable accuracy. Many of the heavy ash particles fall out within less than 200km distance of the eruption (Rose et al., 1995). For more sophisticated approaches, (3) the user may also choose other

aerosol options (GOCART bulk option as well as the MADE/SORGAM or MADE/VBS modal option). For these more complex aerosol options, the finest three ash bins – depending on their size - are added to a "p2.5" (total mass if using GOCART, otherwise split into accumulation and Aitken mode) and a "p10" variable, that are defined as unspeciated aerosols. Using these more complex options enables the capability to include volcanic aerosol interaction with radiation (shortwave as well as long wave) and cloud microphysics. These options also include dry deposition, which follows the descriptions given in the original papers (Grell et al. 2005, Fast et al. 2006). The physical and numerical treatment of this interaction (whether using sections, modes, or total mass only) parallels the existing WRF-Chem inclusion of direct aerosol forcing detailed in Fast et al. (2006) and Barnard et al. (2010) for the MOSAIC (Model for Simulating Aerosol Interactions and Chemistry) sectional 8-bin approach. As above, mass concentrations within the lowest 3 volcanic size bins are first mapped onto the corresponding MOSAIC bins between 2.5 and 10 μm dry diameter. Few data on the microphysical properties of volcanic ash exist to date. Lathem et. al (2011) analyzed the hygroscopic properties of ash originating from 6 different eruptions for ash with diameters less than 125 μm. They concluded a lower hygroscopicity for ash when compared to atmospheric mineral dust aerosol and clays due to the molecular structure of the ash particles. Within this version of the WRF-Chem model, the optical and hygroscopic properties of the volcanic aerosol are assumed to be the same as generic crustal derived dust with a hygroscopicity κ=0.1. As in Fast et al. (2006), Mie calculations are performed for each MOSAIC size bin to calculate aerosol extinction, single scattering albedo, and the asymmetry parameter at 4 wavelengths (300, 400, 600 and 999 nm), with bin summation or extinction weighted averaging used to derive the integrated parameters. Wavelength interpolation based on Ångström coefficients for these 3 quantities is used as input for two radiative transfer options within WRF-Chem (the WRF Rapid

Radiative Transfer Model (RRTMG, Iacono et al., 2008), or the Goddard shortwave scheme, Chou et al., 1998).

Additionally, SO_2 emissions are added to the gas-phase SO_2 variable, if SO_2 is available for the chosen chemistry option. The lifetime of SO_2 is a few days depending on the atmospheric humidity and the amount of hydroxyl (OH) radicals. Typically most of the SO_2 oxidizes in clouds, some SO_2 reacts with OH radicals and is converted to sulfuric acid, H_2SO_4. The calculation of SO_2 requires choosing a WRF-Chem gas-phase chemistry option (Grell et al, 2005). These much more complex chemistry setups come with a heavy computational burden (the most complex setups can easily cost up to a factor of 10 more computational time than just WRF by itself, or WRF with only 4 ash variables but no chemistry), more sophisticated studies of the impact of volcanic eruptions on air quality, weather, and short term climate can be undertaken.

While the emissions preprocessor provides not only volcano location, but also total mass and injection height, the latter will most often be overwritten by the user in the WRF-Chem namelist, assuming that observations are available that are much closer to the truth. For historic cases with known injection heights h and duration d of an eruption, the default initialization parameters are then replaced by the total erupted mass m (kg), which is empirically derived from h (meters) and d (seconds) according to Mastin et al., (2009):

$$m = \rho\, d\, (0.0005\, h)^{4.1494} \qquad (1)$$

The variable ρ denotes the assumed magma density of 2600 kgm^3. Figure 3 shows the mass eruption rate m/d in (kg/sec) derived from equ. 1, which increases significantly with injection height. It is evident that the total mass strongly depends on accurate injection heights. A 500 m error in h at an assumed injection height of 5 km amounts to a mass eruption rate error of about 40 tons per second;

the same 500 m error increases to 1400 tons per second at an injection height of 15 km.

The model results of the impact of an eruption are obviously very sensitive to correct estimates of the plume characteristics. Data assimilation methods have been developed to improve the accuracy of the modeled state of the atmosphere and its composition. It is important to note that WRF offers options to apply three and four dimensional data assimilation. In the case of volcanic emissions, satellite retrievals of characteristics of the ash and SO_2 (i.e. concentrations, aerosol optical depth, chemical composition) may be useful to correct for possible uncertainties in initial mass estimates or plume characteristics through data assimilation methods.

4. Initial applications

The following simulations were produced with a developmental version of WRF-Chem 3.3.1 (Grell et al. 2005) which employs the Advanced Research WRF dynamical core (ARW, Skamarock et al., 2005) with the following parameterizations of physical processes: Mellor-Yamada-Janjić (MYJ) boundary layer parameterization (Janjić, 2002); Noah land-surface model (Chen and Dudhia, 2001); Grell-Devenyi convective parameterization (Grell and Devenyi, 2002); WRF Single-Moment-5 (WSM-5) microphysics (Hong et al., 2004); Goddard shortwave radiation scheme (Chou et al., 1998); Rapid Radiative Transfer Model longwave radiation (RRTM, Mlawer et al., 1997). For the results displayed below, no chemical reactions are taking place. In all simulations WRF-Chem is run with 10 volcanic ash grain-size bins, including grid (advection and diffusion) and sub-grid transport processes (boundary layer vertical mixing, parameterized deep convection), as well as wet deposition, and settling of ash.

4.1 The prediction of ash fall

To show the capability of the model to predict ash-fall, we chose to simulate the 1989 Redoubt eruption in Alaska; see Casadevall (1994) and Miller and Chouet (1994) for more information on the eruption. Some observations of tephra fall deposits were available to us for this period (see Scott and McGimsey, 1994). Although this was also an interesting case for transport of volcanic ash – a KLM B747 briefly lost all of its engines when flying through the ash cloud (Casadevall, 1994) – upper air observational data were not available. To show the transport properties of the modeling system, we therefore decided to use the Eyjafjallajökull volcano in another application presented in the next subsection.

For Redoubt 1989, we focus on the first 2 major explosive eruptions. Miller and Chouet (1994) reported the first eruption at 18:47 with a 10 minute duration, and the second eruption was observed at 19:09 UTC lasting about 13 minutes. For the WRF-Chem initialization, we combined the 2 eruptions in one 23 minute eruption starting on Dec 14, 1989, 19:00 UTC. An injection height of more than 10 km above sea level was reported for the 2 eruption events, thus we used an assumed injection height of 12 km for the WRF-Chem initialization. A 13x13 km^2 horizontal resolution domain is employed, covering Alaska from 162ºW-144ºW longitude and 55ºN-65ºN latitude. The S2 particle size distribution is used (Table 2). The initial and boundary meteorological fields for the WRF-Chem run were derived from the National Centers for Environmental Prediction (NCEP) North American Regional Reanalysis project (http://www.esrl.noaa.gov/psd/data/gridded/data.narr.html). WRF-Chem, with its setup described above, was started at Dec 14 1989, 00:00 UTC, and run for a 48 hour period. Fig. 4 compares results of the total ash-fall predictions with observations of tephra deposited from 14 to 15 December 1989. WRF-Chem seems to capture the dynamic pattern of the ash-fall well when compared with the measured the tephra deposits. The volcanic ash in WRF-Chem was injected at an altitude where winds were predictable over the short time

periods that we are studying. However, the magnitudes of the predicted tephra fall deposits were partly smaller than the observed data. We address this discrepancy first to the large uncertainty of the total mass injected as well as the uncertainty of the assumed size distribution (Carey and Sigurdsson, 1982). Forty percent of the S2 type particle distribution amounts to particles less than 63 μm; chosing a higher share of larger particles would increase the ash fall. In addition there are no aggregation effects included in the model.

4.2 Simulation of ash transport for Eyjafjallajökull

Next we show results from WRF-Chem runs of the Eyjafjallajökull Volcano in Iceland, April of 2010. We initialized WRF-Chem with the meteorological fields from the NCEP FNL (Final) operational global analysis data, which are available on 1.0x1.0 degree grids and are prepared operationally every six hours. A 18x18 km² horizontal resolution domain was employed, covering an area over 5400x3600 km² from Greenland in the NW to the Mediterranean Sea and Turkey in the SE. The domain extends vertically over 35 WRF levels. A detailed evaluation of this case is presented in Webley et al., 2012. WRF-Chem was initialized with volcanic plume altitudes derived from the local weather radar station (IMO, 2010). Two sets of runs were performed using a S1 and a S2 ESP type particle size distribution (compare Table 2), and a source mass according to equ. 1.

The IMO radar heights indicate a continuous eruption starting with a plume height of 9km the 14 April at 9:00 UTC. The WRF-Chem plume heights vary stepwise between 9km and 4km representing mean upper limits of the IMO radar heights. Table 3 shows the plume height and duration used for WRF-Chem; Webley et al (2012) give a detailed description of the used plume characteristics (their figure 2, table 1). Twenty-four hour model simulations are performed from April 14, 00:00 UTC for 5 days until April 19, 00:00 UTC. Each daily model run is re-initialized with the NCEP FNL meteorological data, the WRF-Chem ash output from the previous day, and the corresponding volcanic plume heights. Figure 5

shows the Eyjafjallajökull ash cloud dispersing initially towards the east and southeast extending over Central Europa on the 15 April. The ash dispersed further over Europe and to the east towards northern Russia during the following days, and shifting winds over the North Atlantic from the 18 to 19 April 2010 dispersed ash to the West, south of Greenland. The WRF-Chem runs using the S2 particle size distribution resulted in ash concentrations over Central Europe between 0.5 – 2 mg/m^3 at altitudes between 4 and 6 km km (Webley et al., 2012). Devenish et al. (2012) emphasize that the distance traveled by the ash cloud is clearly sensitive to the size of the ash particles; their simulations with the NAME model show best coincidence of the modeled distal cloud with observational data assuming that less than 5% of the total erupted mass was smaller than 63 μm. The S2 particle size distribution amounts to 40% of the mass within the small bins smaller than 63 μm. Thus with this (S2) distribution and without modeled aggregation, we could expect to overestimate the distal ash cloud. However the S2 WRF-Chem results show reasonable amounts of ash within the distal cloud, which are comparable to observations. The S1 particle size distribution, with 10% of the total mass within the size bins smaller than 63 μm, results in distal clouds with general very similar structures; the total airborne mass (within the domain) amounted to about 20% of the S2 runs. Figure 5 gives snapshots of the development of the ash cloud from April 15-18, and compares the model results using the 2 different size distributions. The S1 runs clearly show a strongly reduced ash loading. We compared the modeled concentrations with satellite volcanic ash retrievals and LIDAR measurements at several measurement locations in Europe (Webley et al., 2012). For Leipzig, the LIDAR showed an ash layer around 4 km ASL passing over the region from 13:47 – 15:32 UTC on April 16, 2010 (Figure 6a). WRF-Chem showed an ash cloud pass over Leipzig between 10:00 and 15:00 UTC. The cloud was around 5 km ASL as it first passed over the site and closer 3 km ASL by the end (Figure 6b). Ash concentrations at around 11:00 UTC reached 800 μg/m^3 (0.8 mg/m^3). A vertical profile to coincide with the LIDAR data (Figure 6c) showed an ash layer from 2 – 4

km ASL with a peak the concentration at 3.5 km ASL. Ansmann et al. (2010) showed from post-processed LIDAR data that the cloud was centered at 3.5 km and had ash concentrations around 900 $\mu g/m^3$. The WRF-Chem modeled magnitude (using the S2 size distribution) proved to be close to the LIDAR data, and the modeled vertical extent of the ash was well comparable to the LIDAR measurements.

5. The software

The software tool necessary to produce the input data to WRF-Chem simulates the movement of volcanic ash-cloud and/or SO_2 is the PREP-CHEM-SRC emission tool (Freitas et al., 2011). This system is coded using Fortran90 and C and requires Hierarchical Data Format (HDF) and Network Common Data Format (NetCDF) libraries. The desired grid configuration and emission inventories to provide emission fluxes and additional information are defined in a Fortran *namelist* file called "prep-chem-src.inp". The software has been tested with GFortran, Intel and Portland Fortran compilers under the UNIX/LINUX operating system. Emissions output from the PREP-CHEM-SRC program are provided in separate intermediate binary data files for volcanic emissions as well as anthropogenic emissions, biomass burning and GOCART aerosol background fields if so desired.

A utility program, convert_emiss, is provided with the WRF-Chem model that converts these separate intermediate files from PREP-CHEM-SRC into WRF input data files. This utility program reads the volcanic emissions binary data file, computes the vertical mass distribution and the emissions for the volcanic ash size bin before populating the emissions input data arrays. The WRF-Chem model then reads the input data and then either re-computes the emissions based upon a new eruption height and vertical mass distribution provided as a WRF-Chem input parameter, or uses the prescribed volcanic ash emissions.

6. Summary and conclusions

A volcanic eruption plume model was added successfully to WRF-Chem. Several options are available in WRF-Chem to treat the transport and fall out of volcanic ash. Initial implementations include options to study the long-range dispersion of small ash particles smaller than 63 μm using only 2 to 4 ash-bin variables. In order to model ash deposition as well as atmospheric transport of ash, subsequently 10 ash variables were added to WRF-Chem describing the typical bin size distribution of the total ash during a volcanic eruption event.

The total ash is distributed into the model bins according to a typical particle distribution scheme, which is characteristic for each eruption type. During an eruption event, the ash is distributed in an umbrella-shape vertical distribution plume above the volcano. Eruption source parameters have been compiled from historic eruptions (Mastin et al., 2009); the source parameters are characteristic for certain eruption types, and have been assigned to 1535 volcanoes worldwide. The parameters were implemented as a look-up table in the WRF-Chem PREP-CHEM-SRC emission tool. The data include injection heights and the duration of an event, and represent the best initial assessment of the type and size of future eruptions. In addition to ash, volcanic SO_2 sources were added from the AEROCOM program. Alternatively to the AEROCOM dataset, SO_2 was implemented in WRF-Chem by distributing SO_2 in an umbrella shaped plume in similar fashion to the ash. The SO_2 initial mass is also estimated as a first guess.

This implementation offers opportunities for the operational community to use this tool for prediction of hazardous evens. WRF-Chem results in mass concentrations of ash, which are useful for ash advisories; most offline Lagrangian models describe the particle trajectory and additional assumptions are needed to derive mass concentrations of ash. Additionally scientists may try to improve their

understanding of the interaction of volcanic aerosols with radiation and microphysics. We plan to test WRF-Chem for near-real time experimental WRF-Chem volcanic ash emission forecasts for modeling domains within the Anchorage Volcanic Ash Advisory Center (http://vaac.arh.noaa.gov/). Once the meteorological source and boundary fields are created, a WRF-Chem run with 10 ash particle size bins takes about 25 minutes using 64 2.6 GHz AMD Opteron processors, and a modeling domain with a 12 kilometer horizontal resolution, 300 by 300 horizontal grid cells (3600x3600 kilometers), and 50 vertical levels; the experimental runs calculate gravitational settling and wet deposition of ash.

Studies with different volcanic ash source models are in progress to test the sensitivity of the various eruption source parameters. Initial model runs of the 1989 Redoubt eruption and the 2010 Eyjafjallajökull eruption showed promising results. The distal ash cloud during the 2010 event was well comparable with satellite remote sensing data and LIDAR measurements. Grell and Baklanov (2011) indicate that the vertical motion fields in the atmosphere may exhibit very large variabilities, which are especially challenging to simulate with offline models. WRF-Chem resulted in a vertically confined ash cloud, which compared well with the shown LIDAR measurements from Leipzig. Obviously the initial ash particle size distribution and the associated mass are critical for the downwind ash concentrations. So far there is no aggregation of volcanic ash particles included in WRF-Chem, although Sparks et al (1997) state that most of the fine ash typically aggregates. We currently most likely overestimate concentrations of fine ash afar from the erupting volcano without considering the effects of aggregation. Future work is needed and online models such as WRF-Chem will facilitate the implementation of parameterization schemes for aggregation of ash particles as described by Costa et al (2010).

Acknowledgements

The authors acknowledge support from the US Air Force Weather Agency and the University of Alaska Arctic Region Supercomputing Center. This publication results in part of research sponsored by the Cooperative Institute for Alaska Research with funds from the National Oceanic and Atmospheric Administration under cooperative agreement NA08OAR4320751 with the University of Alaska. S. R. Freitas acknowledges partial support of this work by CNPq (302696/2008-3). We would like to thank Larry Mastin and an anonymous reviewer for their comments.

References

Ackermann, I. J., Hass, H., Memmesheimer, M. , Ebel, A., Binkowski, F. S. , and Shankar, U.: Modal aerosol dynamics model for Europe: Development and first applications, Atmos. Environ., 32, 2981-2999, 1998.

Ahmadov, R., McKeen, S. A., Robinson, A., Bahreini, R., Middlebrook, A., de Gouw, J., Meagher, J., Hsie, E., Edgerton, E., Shaw, S., and Trainer, M.: A volatility basis set model for summertime secondary organic aerosols over the eastern United States in 2006, J. Geophys. Res., 117, D06301, doi:10.1029/2011JD016831, 2012.

Albrecht, B. A.: Aerosols, cloud microphysics, and fractional cloudiness, Science, Vol. 245 no. 4923 pp. 1227-1230, 1989

Ansmann, A., Tesche, M., Groß, S., Freudenthaler, V., Seifert, P., Hiebsch, A., Schmidt, J., Wandinger, U., Mattis, I., Müller, D., and Wiegner, M.: The 16 April 2010 major volcanic ash plume over central Europe: EARLINET lidar and AERONET photometer observations at Leipzig and Munich, Germany, Geoph. Res. Let., 37, L13810, doi:10.1029/2010GL043809, 2010.

Barnard, J., Fast, J., Paredes-Miranda, G., Arnott, W., and Laskin, A.: Technical Note: Evaluation of the WRF-Chem "Aerosol Chemical to Aerosol Optical Properties" Module using data from the MILAGRO campaign, Atmos. Chem. Phys., **10,** 7325-7340, 2010.

Bonadonna, C., Mayberry, G.C., Calder, E.S., Sparks, R.S.J., Choux, C., Jackson, A.M., Lejeune, A.M., Loughlin, S.C., Norton, G.E., Rose, W.I., Ryan, G., Young, S.R.: Tephra fallout in the eruption of Soufrière Hills Volcano, Montserrat. In: Druitt, T.H., Kokelaar, B.P. (Eds.), The eruption of Soufrière Hills Volcano, Montserrat, from 1995 to 1999, Geological Society of London, London, pp. 483–516, 2002.

Bonadonna, C., Houghton, B.F.: Total grain-size distribution and volume of tephrafall deposits, Bul. Volc. 67, 441–456, 2005.

Bulletin of the Global Volcanism Network (BGVN. Weekly report of Puyehue-Cordón Caulle volcano, 1 June - 7 June 2011. Viewed on July 9, 2012. http://www.volcano.si.edu/world/volcano.cfm?vnum=1507-15=&volpage=weekly, 2011.

Carey, S. N., and Sigurdsson, H.: Influence of particle aggregation on deposition of distal tephra from the May 18, 1980, eruption of Mount St. Helens volcano, J. Geoph. Res., 87(B8), 7061–7072, 1982.

Casadevall, T. J.: The 1989/1990 eruption of Redoubt Volcano Alaska: impacts on aircraft operations. Journal of Volcanology and Geothermal Research. 62 (30). 301- 316, 1994.

Chapman, E. G., Gustafson Jr., W. I. , Easter, R. C., Barnard, J. C. , Ghan, S. J. , Pekour, M. S. , and Fast, J. D.: Coupling aerosol-cloud-radiative processes in the WRF-Chem model: Investigating the radiative impact of elevated point sources, Atmos. Chem. Phys., 9, 945-964, 2009.

Chen, F., and Dudhia, J.: Coupling an advanced land-surface/hydrology model with the Penn State/NCAR MM5 modeling system. Part I: Model description and implementation, Mon. Wea. Rev. 129: 569-585, 2001.

Chin, M., Ginoux, P., Kinne, S., Holben, B. N., Duncan, B. N., Martin, R. V., Logan, J., Higurashi, A., and Nakajima, T.: Tropospheric aerosol optical thickness from the GOCART model and comparisons with satellite and sunphotometer measurements, J. Atmos. Sci. 59, 461-483, 2002.

Chou, M. D., Suarez, M. J. , Ho, C. H., Yan, M. M. H. , and Lee, K. T.: Parameterizations for cloud overlapping and shortwave single-scattering properties for use in general circulation and cloud ensemble models, J. Clim., 11, 202– 214, 1998.

Costa, A., Folch A., and Macedonio G.: A model for wet aggregation of ash particles in volcanic plumes and clouds: 1. Theoretical formulation, J. Geophys. Res., 115, B09201, doi:10.1029/2009JB007175, 2009.

Devenish, B. J., Francis P. N., Johnson B. T., Sparks R. S. J., and Thomson D. J.: Sensitivity analysis of dispersion modeling of volcanic ash from Eyjafjallajökull in May 2010, J. Geophys. Res., 117, D00U21, doi:10.1029/2011JD016782, 2012.

Diehl, T.: A global inventory of volcanic SO_2 emissions for hindcast scenarios, (http://www-lscedods.cea.fr/aerocom/AEROCOM_HC/), 2009.

Diehl, T., et al.: A global inventory of subaerial volcanic SO_2 emissions from 1979 to 2008, in preparation, 2012.

Durant, A. J., and Rose, W. I.: Sedimentological constraints on hydrometeor-enhanced particle deposition: 1992 Eruptions of Crater Peak, Alaska, J. Volcanol. Geotherm. Res. 186: 40-59, doi:10.1016/j.jvolgeores.2009.02.004, 2009.

Durant, A.J., Rose, W.I., Sarna-Wojcicki, A.M., Carey, S. and Volentik, A.C.: Hydrometeor-enhanced tephra sedimentation: Constraints from the 18 May 1980 eruption of Mount St. Helens (USA). J. Geoph. Res. doi:10.1029/2008JB005756, 2009.

Fast, J. D., Gustafson Jr., W. I., Easter, R. C., Zaveri, R. A., Barnard, J. C., Chapman, E. G., Grell, G. A., and Peckham, S. E.: Evolution of ozone, particulates, and aerosol direct radiative forcing in the vicinity of Houston using a fully coupled meteorology-chemistry-aerosol model, J. Geophys. Res., 111, D21305, doi:10.1029/2005JD006721, 2006.

Freitas, S. R., Longo, K. M., Silva Dias, M. A. F., Chatfield, R., Silva Dias, P., Artaxo, P., Andreae, M. O., Grell, G., Rodrigues, L. F., Fazenda, A., and Panetta, J.: The Coupled Aerosol and Tracer Transport model to the Brazilian developments on the Regional Atmospheric Modeling System (CATT-BRAMS) – Part 1: Model description and evaluation, Atmos. Chem. Phys., 9, 2843-2861, 2009.

Freitas, S. R., Longo, K. M., Alonso, M. F., Pirre, M., Marecal, V., Grell, G., Stockler, R., Mello, R. F., and Sánchez Gácita, M.: PREP-CHEM-SRC – 1.0: a

preprocessor of trace gas and aerosol emission fields for regional and global atmospheric chemistry models, Geosci. Model Dev., 4, 419-433, doi:10.5194/gmd-4-419-2011, 2011.

Grell, G. A., and Devenyi, D.: A generalized approach to parameterizing convection combining ensemble and data assimilation techniques, Geoph. Res. Let. 29(14): 1693, doi:10.1029/2002GL015311, 2002.

Grell, G. A., Peckham, S. E., Schmitz, R., McKeen, S. A., Frost, G., Skamarock, W. C., Eder, B.: Fully coupled 'online' chemistry within the WRF model, Atm. Env., 39, 37, 6957-6975, 2005.

Grell, G.A., and Baklanov, A.: Integrated Modeling for Forecasting Weather and Air Quality: A Call for Fully Coupled Approaches, Atmos. Env.,. Doi: 10.1016/j.atmosenv.2011.01.017, 2011

Grell, G., Freitas, S. R., Stuefer, M., and Fast, J.: Inclusion of biomass burning in WRF-Chem: impact of wildfires on weather forecasts, Atmos. Chem. Phys., 11, 5289-5303, doi:10.5194/acp-11-5289-2011, 2011.

Grell, G. A., Fast, J., Gustafson, W. I., Peckham, S. E., McKeen, S. A., Salzmann, M., and Freitas, S.: On-Line Chemistry within WRF: Description and Evaluation of a State-of-the-Art Multiscale Air Quality and Weather Prediction Model, in Integrated Systems of Meso-Meteorological and Chemical Transport Models, edited by A. Baklanov, A. Mahura and R. Sokhi, Springer, 2011.

Gudmundsson, M. T., Pedersen, R., Vogfjörd, K., Thorbjarnardóttir, B., Jakobsdóttir, S., and Roberts, M. J.: Eruptions of Eyjafjallajökull Volcano, Iceland. Eos, 91 (21), 190-191, 2010.

Gustafson Jr., W. I., Chapman, E. G., Ghan, S. J., Easter, R. C., Fast, and J. D.: Impact on Modeled Cloud Characteristics Dueto Simplified Treatment of Uniform Cloud Condensation Nuclei During NEAQS 2004, Geophys. Res. Lett., 34, L19809,doi:10.1029/2007GL030021, 2007.

Hong, S.Y., Dudhia, J., and Chen, S.H.: A revised approach to ice-microphysical processes for the bulk parameterization of cloud and precipitation, Mon. Wea. Rev., 132, 103-120, 2004.

Iacono, M. J., Delamere, J.S., Mlawer, E.J., Shephard, M.W., Clough, S.A., and Collins, W.D.: Radiative forcing by long-lived greenhouse gases: Calculations with the AER radiative transfer models, J. Geophys. Res., **113**, D13103, doi: 10.1029/2008 JD009944, 2008.

Icelandic Meteorological Office (IMO): Eyjafjallajökull 2010 plume altitude measured by weather radar. http://andvari.vedur.is/~arason/radar/, 2010.

Janjić, Z. I.: Nonsingular implantation of the Mellor–Yamada level 2.5 scheme in the NCEP mesomodel. NOAA/NWS/NCEP Office Note 437, 61 pp., 2002.

Lathem, T. L., P. Kumar, A. Nenes, J. Dufek, I. N. Sokolik, M. Trail, and A. Russell: Hygroscopic properties of volcanic ash, Geophys. Res. Lett., 38, L11802, doi:10.1029/2011GL047298, 2011.

Mastin, L., Guffanti, M., Servranckx, R., Webley, P., Barsotti, S., Dean, K., Durant, A., Ewert, J., Neri, A., and Rose, W.: A multidisciplinary effort to assign realistic source parameters to models of volcanic ash-cloud transport and dispersion during eruptions, J. Volc. and Geoth. Res., 186, 1, 10-21, 2009.

McCormick, M. P., Thomason, L. W., and Trepte, C. R.: Atmospheric effects of the Mt. Pinatubo eruption, Nature, 373, 399 – 404, doi:10.1038/373399a0, 1995.

Miller, T. P., and Chouet, B. A.: The 1989-1990 eruptions of Redoubt volcano: an introduction: in Miller, T. P. and Chouet, B. A., (eds.), The 1989-1990 eruptions of Redoubt Volcano, Alaska, J. Volc. and Geoth. Res., 62, 1, p. 1-10, 1994.

Mlawer, E. J., Taubman, S. J., Brown, P. D., Iacono, M. J., and Clough, S. A.: Radiative transfer for inhomogeneous atmosphere: RRTM, a validated correlated-k model for the longwave, J. Geoph. Res. 102(D14): 16,663–16,682, 1997.

Pruppacher, H. R., and Klett, J. D.: Microphysics of Clouds and Precipitation, Second edition, Kluwer Academic Publishers, Dordrecht, The Netherlands, 954 pp., 1997.

Rose, W. I., Kostinski, A. B., and Kelley, L.: Real time C band radar observations of 1992 eruption clouds from Crater Peak/Spurr Volcano, Alaska, U.S.G.S. Bulletin 2139 (Spurr Eruption, edited by T. Keith), 19-26, 1995.

Rose, W.I., Self, S., Murrow, P. J., Ernst, G.J., Bonadonna C., and Durant, A.J.: Pyroclastic fall deposit from the October 14, 1974 eruption of Fuego Volcano, Guatemala, Bull Volc., DOI 10.1007/s00445-007-0187-5, 2007.

Salzmann, M.: WRF-Chem/KPP Coupler (WKC) for WRF V3, Users' and Developers Guide v2.0, Princeton University, Princeton, NJ, 2008.

Schell, B., Ackermann, I. J., Hass, H., Binkowski, F. S., and Ebel, A.: Modeling the formation of secondary organic aerosol within a comprehensive air quality modeling system, J. Geophys. Res., 106, 28275-28293, 2001.

Scollo, S., Del Carlo, P., and Coltelli, M.: Tephra fallout of 2001 Etna flank eruption: Analysis of the deposit and plume dispersion, J. Volc. and Geoth. Res. 160, 147–164, 2007.

Scott, W.E. and McGimsey, R.G.: Character, mass, distribution, and origin of tephra-fall deposits of the 1989-1990 eruption of Redoubt Volcano, south-central Alaska. In: T.P. Miller and B.A. Chouet (Editors), The 1989-1990 Eruptions of Redoubt Volcano, Alaska, J. Volcanol. Geotherm. Res., 62:251-272, 1994.

Shrivastava, M., Fast, J.D., Easter, R.C., Gustafson Jr., W.I., Zaveri, R.A., Hodzic, A., and Jimenez, J.: Modeling organic aerosols in a megacity: comparison of simple and complex representations of the volatility basis set approach, Atmos. Chem. Phys., 11, 6639-6662, 2011.

Skamarock, W.C., Klemp J.B., Dudhia, J., Gill, D.O., Barker, D. M., Wang, W., and Powers, J. G.: A description of the advanced research WRF version 2. NCAR Technical Note, NCAR/TN-468+STR, 88 pp., 2005.

Sparks, R.S.J., Bursik, M.I., Carey, S.N., Gilbert, J.S., Glaze, L.S., Sigurdsson, H., and Woods, A.W.: Volcanic Plumes. John Wiley and Sons, Sussex, 574 pp., 1997.

Stockwell, W. R., Middleton, P., Chang, J. S., and Tang, X.: The second generation regional acid deposition model chemical mechanism for regional air quality modeling, J. Geophys. Res., 95, 16343-16367, 1990.

Twomey, S.: The Influence of Pollution on the Shortwave Albedo of Clouds. J. Atmos. Sci., 34, 1149–1152, 1977.

Webley, P.W. and Mastin, L. G.: Improved Prediction and tracking of Volcanic Ash clouds. Journal of Volcanology and Geothermal Research: Special Issue on Volcanic Ash Clouds, eds. Larry Mastin and Peter Webley. 186 (1 – 2), 1 - 9. doi:10.1016/j.jvolgeores.2008.10.022, 2009.

Webley, P.W., Steensen, T., Stuefer, M., Grell, G. A., Freitas, S., and Pavolonis, M.: Analyzing the Eyjafjallajökull 2010 eruption using satellite remote sensing, lidar and WRF-Chem dispersion and tracking model. J. Geophys. Res., **117**, D00U26, 21 pp., doi:10.1029/2011JD016817, 2012.

World Meteorological Organization (WMO): Workshop on Ash Dispersal forecast and civil aviation: model definition document, viewed April 16, 2011. http://www.unige.ch/sciences/terre/mineral/CERG/Workshop/results/Model-Document-Geneva10.pdf, 2010.

Zaveri, R.A., and Peters, L.R.: A new lumped structure photochemical mechanism for large-scale applications, J. Geophys. Res., 104, 30, 387-30, 415, 1999.

Zaveri R.A., Easter, R.C., Fast, J.D., and Peters, L. K.: Model for simulating aerosol interactions and chemistry, J. Geophys. Res., **113**, D13204, doi:10.1029/2007JD008782, 2008.

Table Captions:

Table 1. Injection height, duration, eruption rate, volume and mass fraction (< 63μm) as provided by Mastin et al. (2009) and used to determine the eruption properties within the WRF-Chem model. Adapted from Mastin et al. (2009).

Table 2. Ash particle bin size ranges with corresponding WRF-Chem variable names; the mass fractions in percent of total mass are given below each ESP eruption type M0-M3 and S0-S9.

Table 3. The duration and height of the Eyjafjallajökull plume used for WRF-Chem for the period from April 14-19, 2010.

Figure Captions:

Figure 1: The vertical profile of the ash-cloud mass distribution (%) associated with an eruption with 12 km height above the vent. In this case, the cloud base is located around 9 km height above the vent. Note the umbrella cloud detrainment layer represented as a parabolic mass distribution with 75% of the erupted mass. The 25% of the erupted mass is linearly detrained from the umbrella base to the vent height.

Figure 2: The global dataset of volcanoes described in Mastin et al. (2009) and included in WRF-Chem model to simulate ash-cloud movement. The figure shows the plume height above the vent prescribed for each volcano with past and potential future eruption.

Figure 3: Mean mass eruption rates derived from injection heights.

Figure 4: Left: measured tephra-fall deposits (g/m^2) from the 1989 eruption of Redoubt Volcano, south-central Alaska, as adapted from Scott and McGimsey (1994). The dotted and dashed contour lines (2, 10, 100, 1000 g/m^2) delineate the isopachs from 14 Dec and 15 December 1989; the measurement locations are indicated with small dots (large dots are geographic reference points). Right: WRF-Chem modeled ash-fall using the same isopach intervals.

Figure 5: Daily WRF-Chem dispersion of the Eyjafjallajökull ash mass loading from 15 April 2010 to the 18 April 2010. The top 3 panels represent WRF-Chem model results using the S1 particle size distribution, the bottom panels represent WRF-Chem results with the S2 particle size distribution.

Figure 6: (A) Earlinet LIDAR at Leipzig, Germany showing the evolution of the major ash plume over Leipzig on April 16, 2010 (in red, 3–5 km height, 13:47–15:32 UTC) in terms of 1064–nm range–corrected (RC) lidar signal (arbitrary units), (B) WRF-Chem simulation from 10:00 – 16:00 UTC and (C, D) vertical profiles at 11:00 and 14:00 UTC respectively (adapted from Webley et al., 2012).

Tables:

Table 1:

ESP	Type	Example	Height above vent (km)	Duration (hr)	Eruption rate (kg/s)	Volume (km^3)	Mass fraction less than 63 micron
M0	Standard mafic	Cerro Negro. Nicaragua. 4/13/1992	7	60	1.00E+05	0.01	0.05
M1	small mafic	Etna. Italy. 7/19-24/2001	2	100	5.00E+03	0.001	0.02
M2	medium mafic	Cerro Negro. Nicaragua. 4/9-13/1992	7	60	1.00E+05	0.01	0.05
M3	large mafic	Fuego. Guatemala. 10/14/1974	10	5	1.00E+06	0.17	0.1
S0	standard silicic	Spurr. USA. 8/18/1992	11	3	4.00E+06	0.015	0.4
S1	small silicic	Ruapehu. New Zealand. 6/17/1996	5	12	2.00E+05	0.003	0.1
S2	medium silicic	Spurr. USA. 8/18/1992	11	3	4.00E+06	0.015	0.4
S3	large silicic	St. Helens. USA. 5/18/1980	15	8	1.00E+07	0.15	0.5
S8	co-ignimbrite silicic	St. Helens. USA. 5/18/1980 (pre-9 AM)	25	0.5	1.00E+08	0.05	0.5
S9	Brief silicic	Soufrière Hills. Montserrat (composite)	10	0.01	3.00E+06	0.0003	0.6
U0	default submarine	none	0	--	--	--	

Table 2:

Particle Size Bin	Phi	WRF Var	M0	M1	M2	M3	S0	S1	S2	S3	S8	S9
1 – 2mm	-1 – 0	vash_1	6.5	0.0	6.5	13.0	22.0	24.0	22.0	2.9	2.9	0.0
0.5 – 1 mm	0– 1	vash_2	12.0	4.0	12.0	20.0	5.0	25.0	5.0	3.6	3.6	0.0
0.25 – 0.5 mm	1– 2	vash_3	18.8	10.0	18.8	27.5	4.0	20.0	4.0	11.8	11.8	0.0
125 – 250 µm	2– 3	vash_4	36.3	50.0	36.3	22.5	5.0	12.0	5.0	8.2	8.2	9.0
62.5 – 125 µm	3– 4	vash_5	20.5	34.0	20.5	7.0	24.5	9.0	24.5	7.9	7.9	22.0
31.25 – 62.5 µm	4– 5	vash_6	3.0	2.0	3.0	4.0	12.0	4.3	12.0	13.0	13.0	23.0
15.625 – 31.25 µm	5– 6	vash_7	1.5	0.0	1.5	3.0	11.0	3.3	11.0	16.3	16.3	21.0
7.8125 – 15.625 µm	6– 7	vash_8	1.0	0.0	1.0	2.0	8.0	1.3	8.0	15.0	15.0	18.0
3.9065 – 7.8125 µm	7– 8	vash_9	0.5	0.0	0.5	1.0	5.0	0.8	5.0	10.0	10.0	7.0
< 3.9 µm	> 8	vash_10	0.0	0.0	0.0	0.0	3.5	0.5	3.5	11.2	11.2	0.0

Table 3:

Start time (UTC)	Duration (hrs)	End time	Height ASL (km)
4/14/10 9:00	10	4/14/10 19:00	9
4/14/10 19:00	9	4/15/10 4:00	5.5
4/15/10 4:00	39	4/16/10 19:00	6
4/16/10 19:00	35	4/18/10 6:00	8.25
4/18/10 6:00	17	4/18/10 23:00	5
4/18/10 23:00	1	4/19/10 0:00	4

Figures:

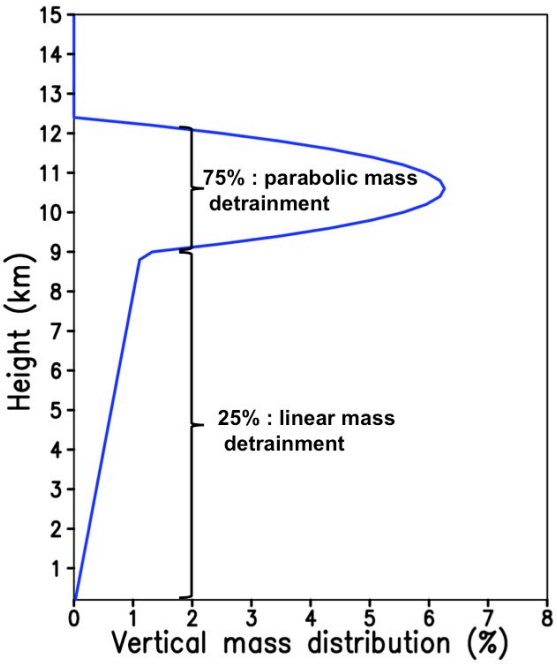

Figure 1

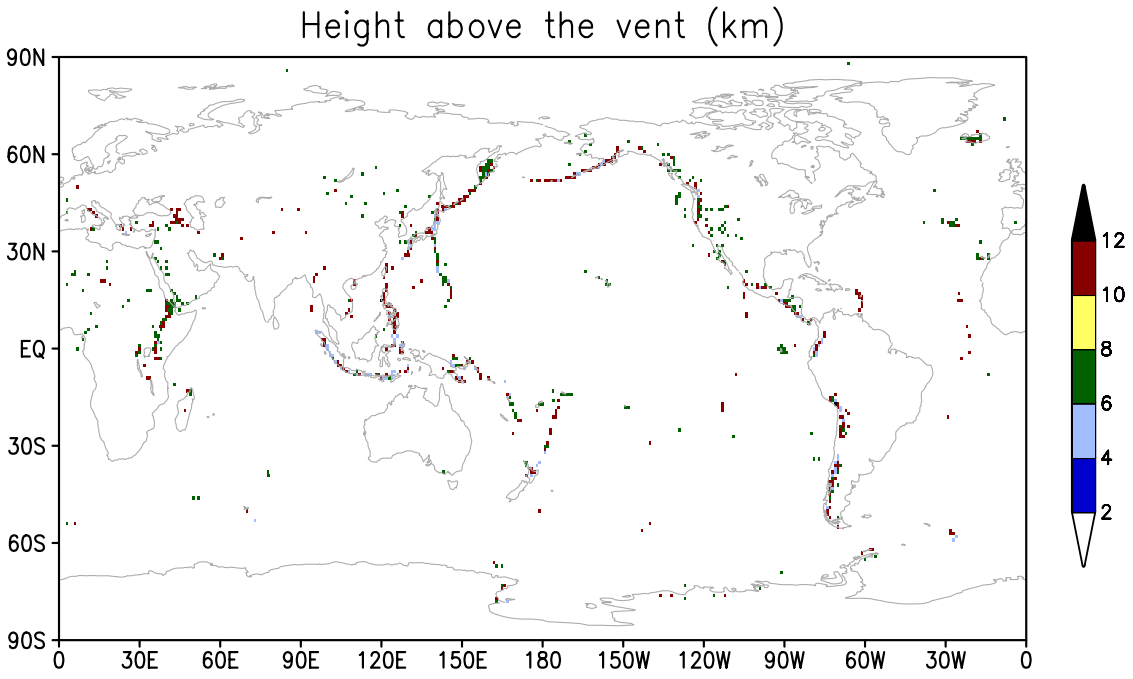

Figure 2

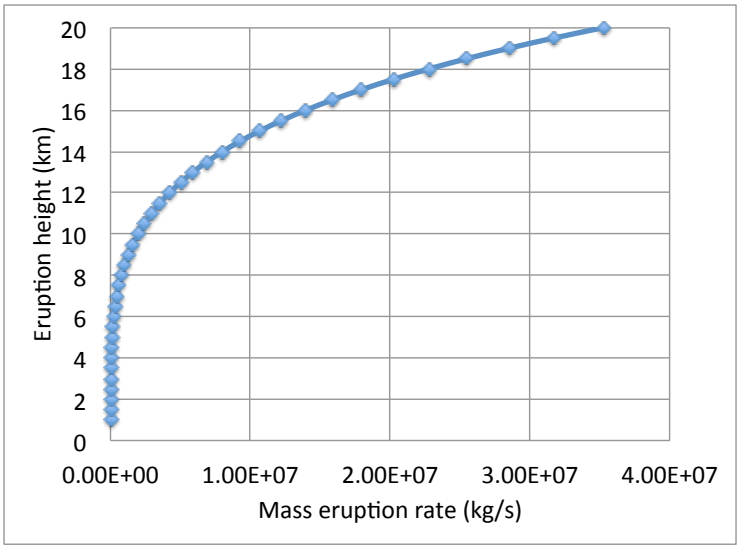

Figure 3

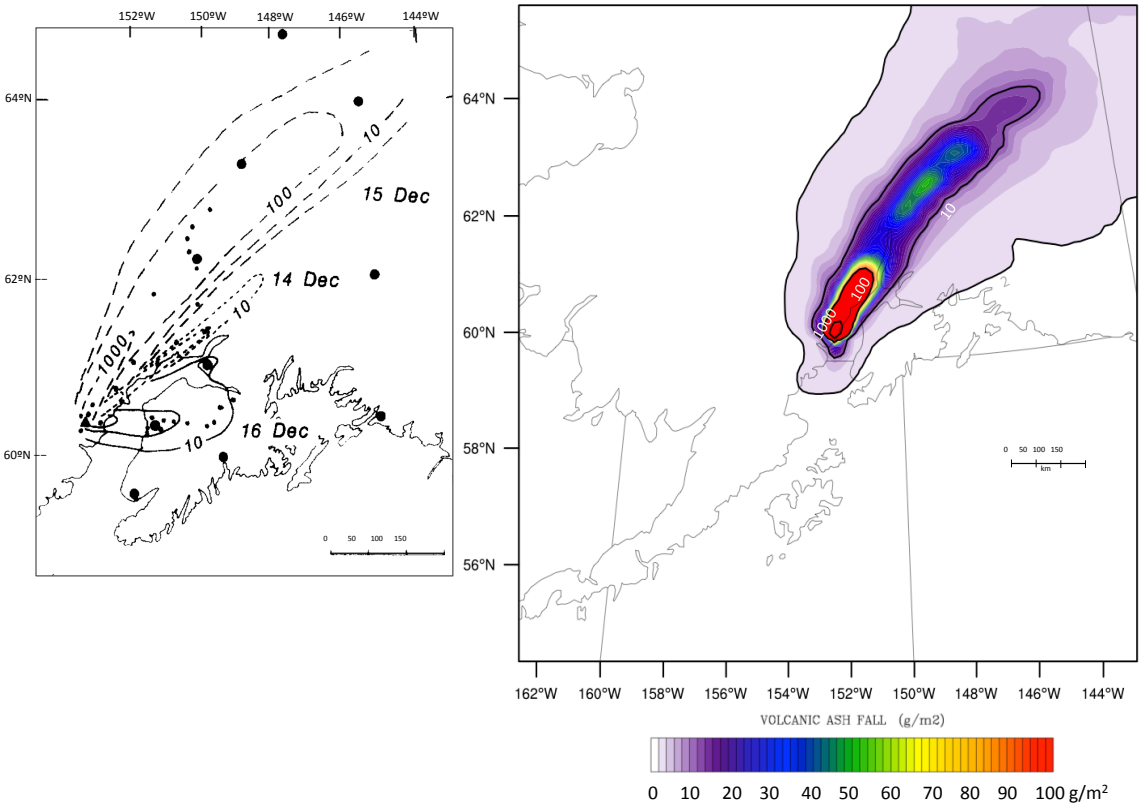

Figure 4

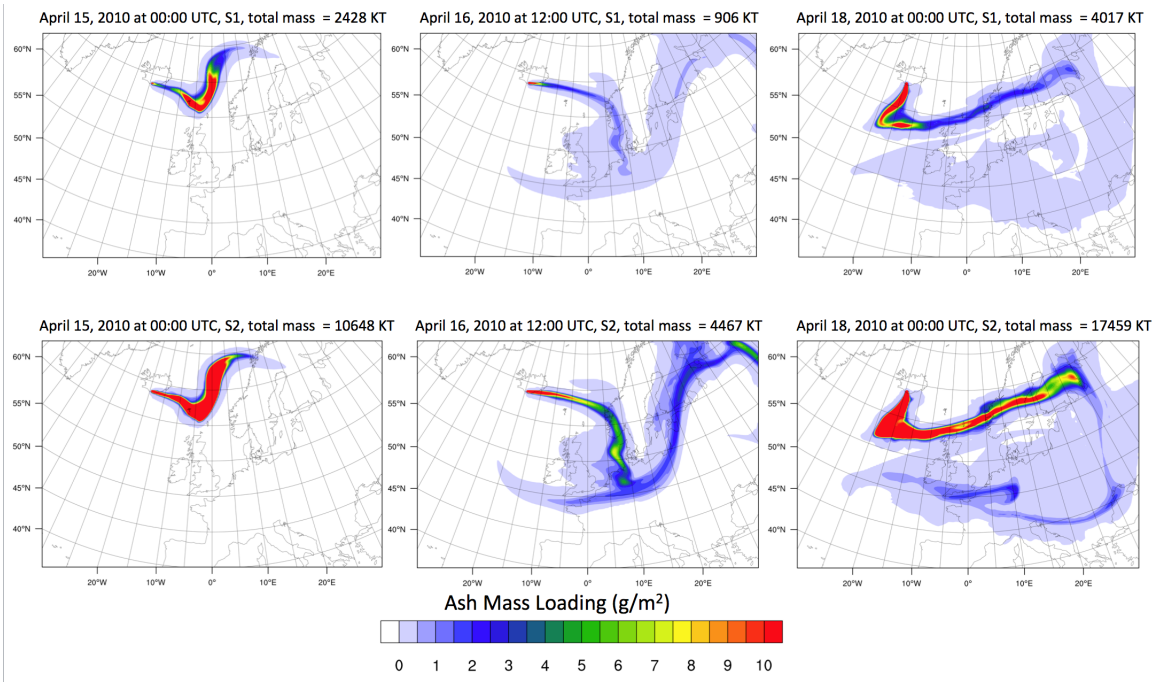
April 15, 2010 at 00:00 UTC, S1, total mass = 2428 KT
April 16, 2010 at 12:00 UTC, S1, total mass = 906 KT
April 18, 2010 at 00:00 UTC, S1, total mass = 4017 KT
April 15, 2010 at 00:00 UTC, S2, total mass = 10648 KT
April 16, 2010 at 12:00 UTC, S2, total mass = 4467 KT
April 18, 2010 at 00:00 UTC, S2, total mass = 17459 KT
60°N
55°N
50°N
45°N
40°N
20°W
10°W
0°
10°E
20°E
Ash Mass Loading (g/m²)
0 1 2 3 4 5 6 7 8 9 10

Figure 5

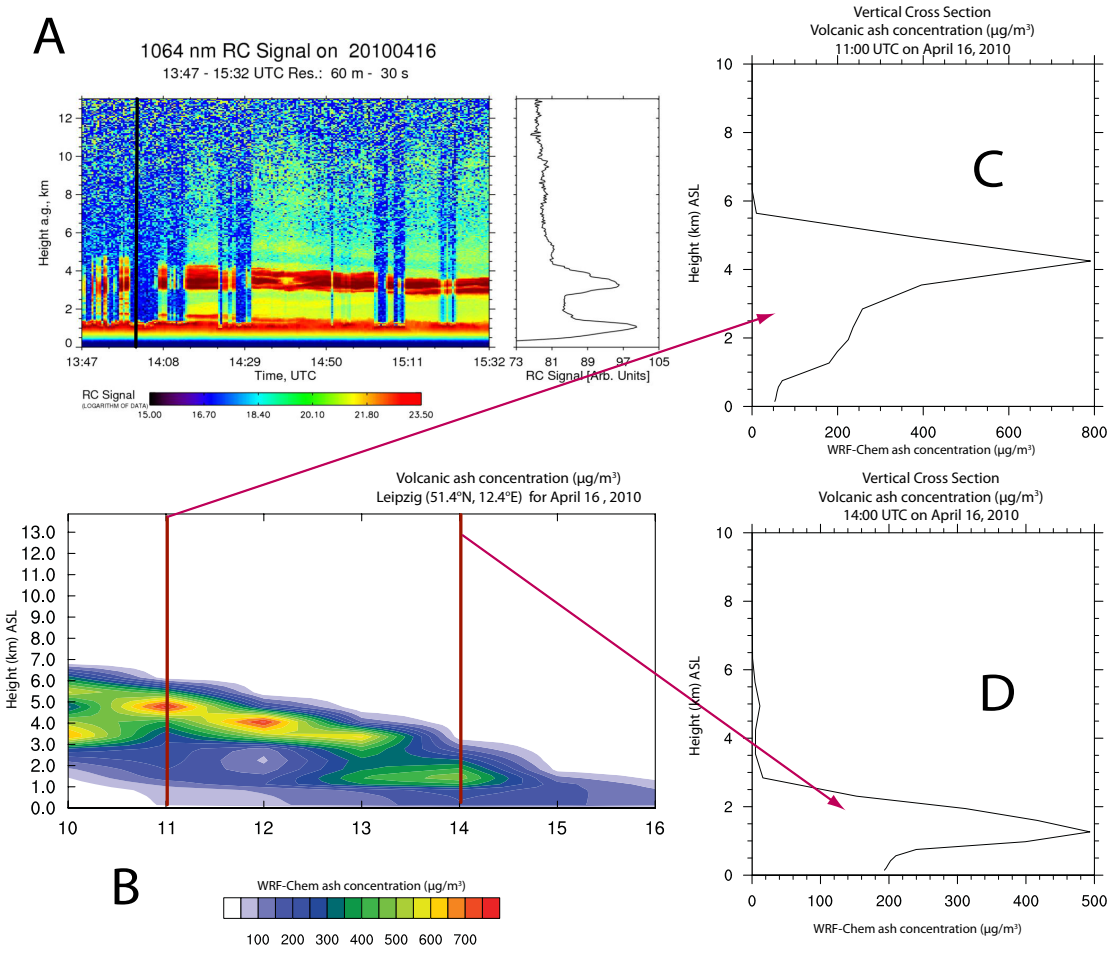
A
1064 nm RC Signal on 20100416
13:47 - 15:32 UTC Res.: 60 m - 30 s
Height a.g., km
Time, UTC
RC Signal [Arb. Units]
RC Signal
Vertical Cross Section
Volcanic ash concentration (µg/m³)
11:00 UTC on April 16, 2010
C
Height (km) ASL
WRF-Chem ash concentration (µg/m³)
Volcanic ash concentration (µg/m³)
Leipzig (51.4°N, 12.4°E) for April 16 , 2010
Height (km) ASL
B
WRF-Chem ash concentration (µg/m³)
Vertical Cross Section
Volcanic ash concentration (µg/m³)
14:00 UTC on April 16, 2010
D
Height (km) ASL
WRF-Chem ash concentration (µg/m³)

Figure 6